Nanomanufacturing
University of Michigan
ME599-002 | Winter 2010

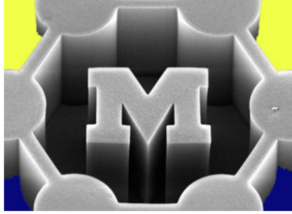

08: **Surface energy, melting, and wetting**

February 8, 2010

John Hart
ajohnh@umich.edu
http://www.umich.edu/~ajohnh

Announcements

- HW2 posted, due M Feb/22

Recap: intermolecular and surface forces

- Electrostatic/polarization interactions cause intermolecular forces, at length scales of 1-100 nm (short-long range)
- We can calculate forces between solid bodies by summing pairwise interaction potentials, e.g., for van der Waals forces using the Lennard-Jones potential
- These forces practically govern adhesion, local deformation, and assembly of nanostructures

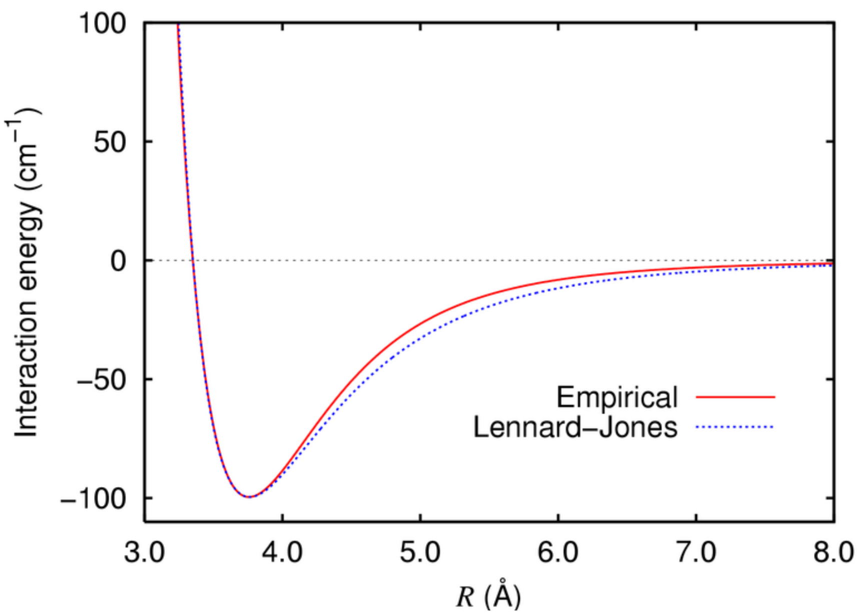

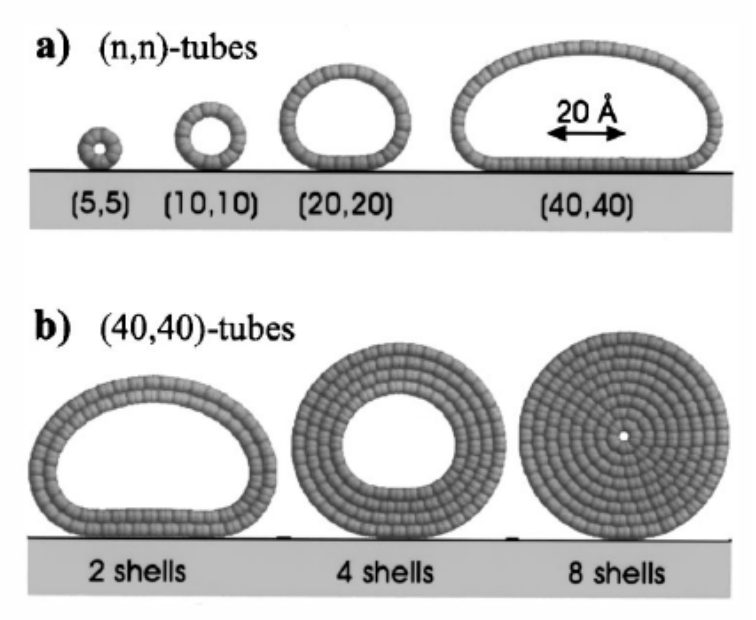

Hertel et al., Physical Review B 58(20):13870, 1998.

VDW energies for regular geometries

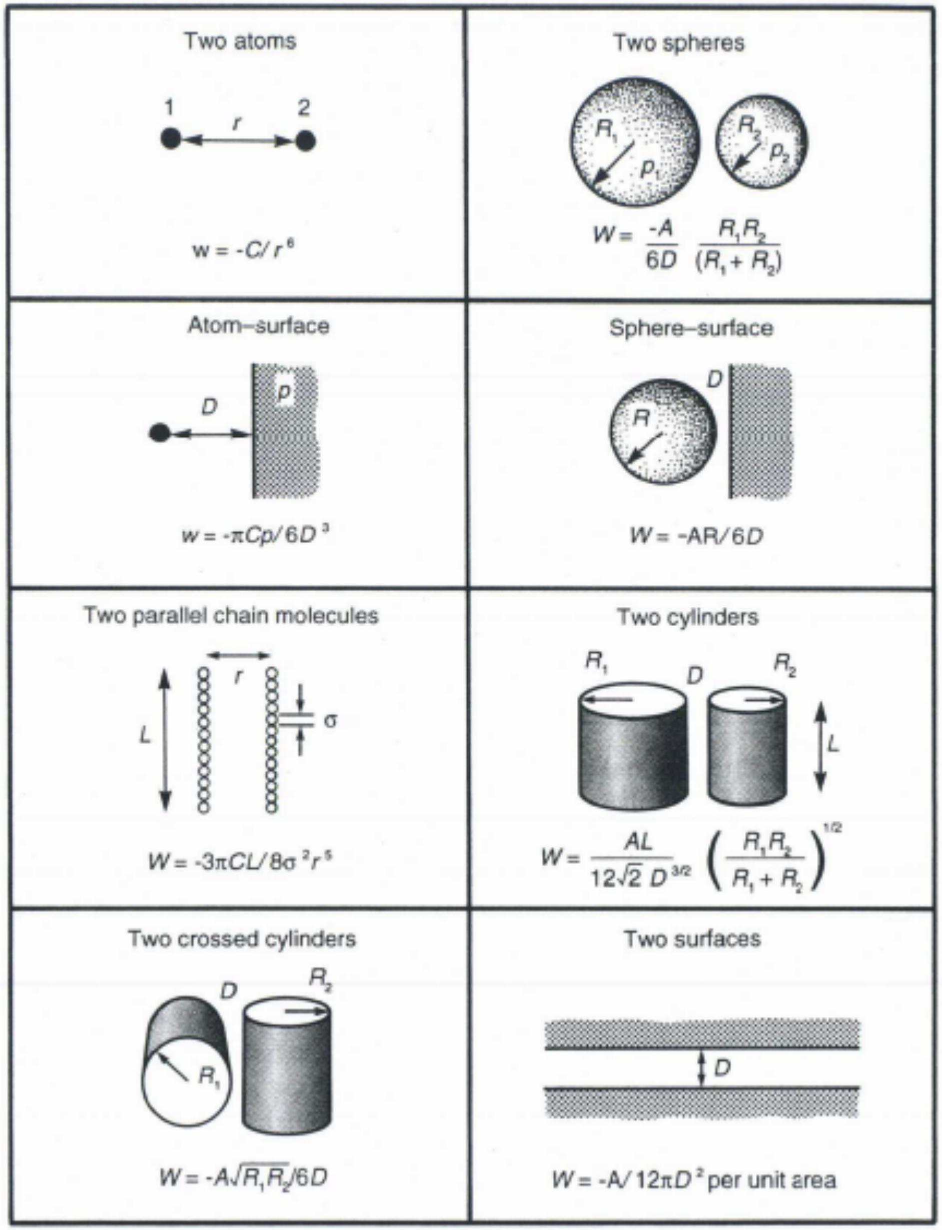

Two atoms $w = -C/r^6$	Two spheres $W = \frac{-A}{6D}\frac{R_1R_2}{(R_1+R_2)}$
Atom–surface $w = -\pi C\rho/6D^3$	Sphere–surface $W = -AR/6D$
Two parallel chain molecules $W = -3\pi CL/8\sigma^2 r^5$	Two cylinders $W = \frac{AL}{12\sqrt{2}\,D^{3/2}}\left(\frac{R_1R_2}{R_1+R_2}\right)^{1/2}$
Two crossed cylinders $W = -A\sqrt{R_1R_2}/6D$	Two surfaces $W = -A/12\pi D^2$ per unit area

Israelachvili.

Adhesion scaling in nature

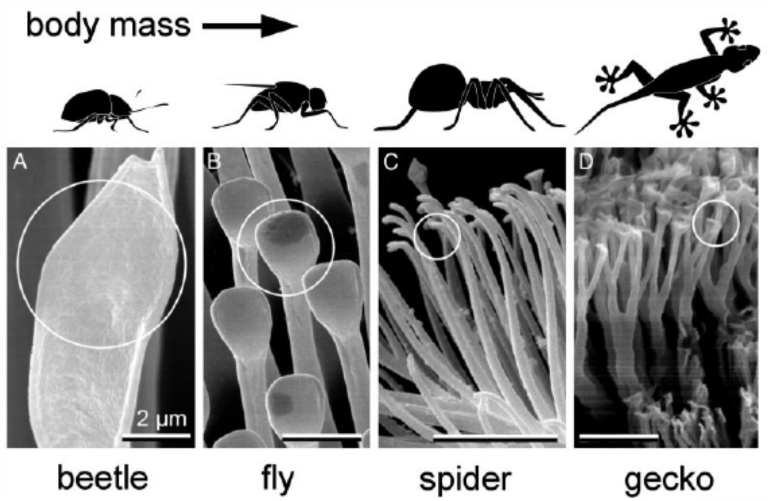

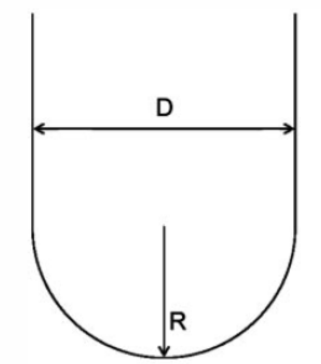

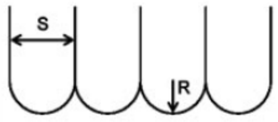

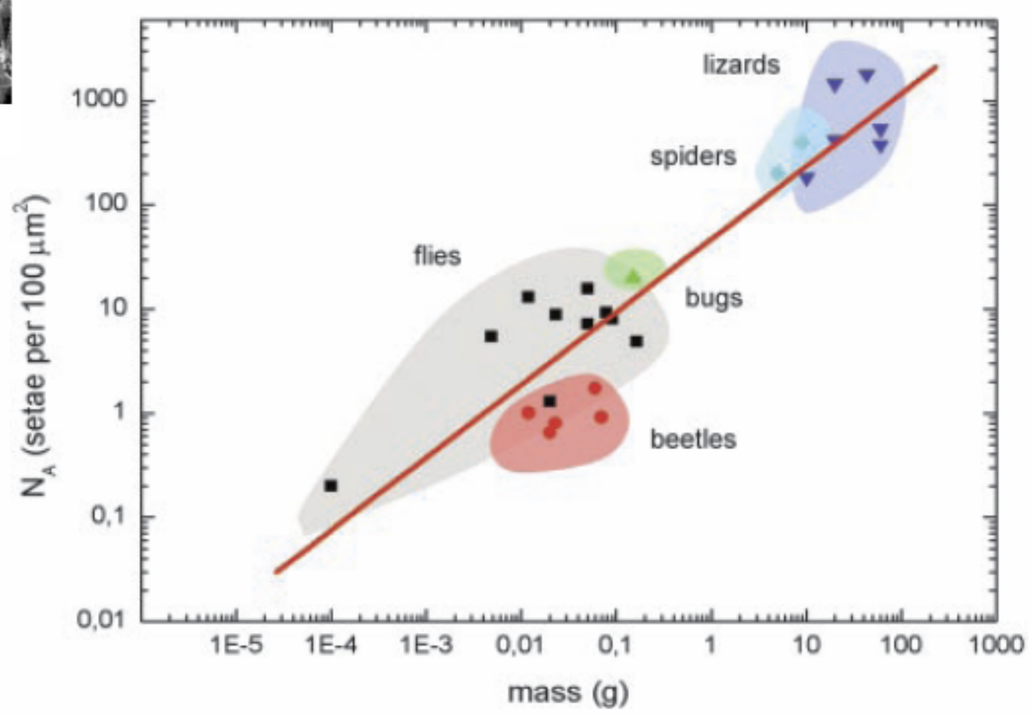

Fig. 2. Dependence of the terminal element density (N_A) of the attachment pads on the body mass (m) in hairy-pad systems of diverse animal groups ($\log \cdot N_A(m^{-2}) = 13.8 + 0.699 \cdot \log \cdot m(kg)$, $R = 0.919$).

Artl et al., PNAS 100(19):10603-10606, 2003.

Synthetic gecko adhesives

Gecko

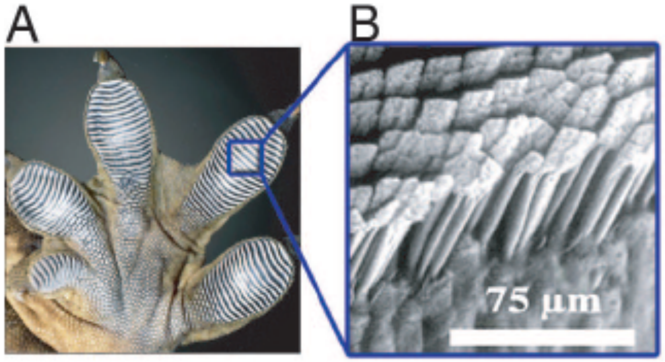

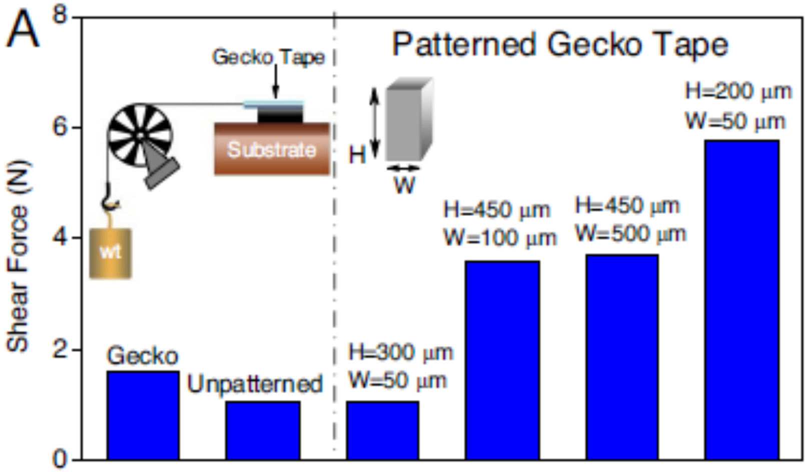

CNTs

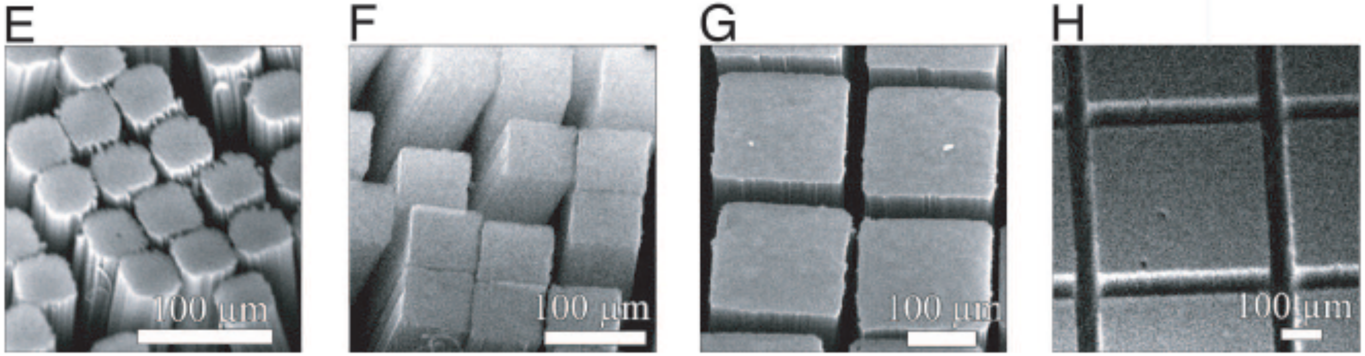

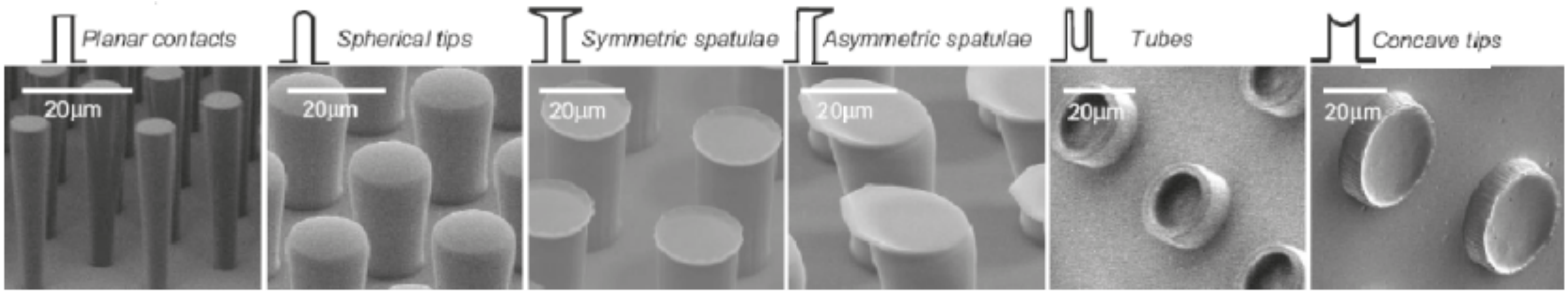

Ge et al., PNAS 104(26):10792-10795, 2007.
Zeng et al., Langmuir 25(13):7486–7495, 2009.

Today's agenda

- Definition of surface energy and work of adhesion
- Thermodynamic model of melting point decrease (suppression) of nanoparticles
- Generalization to different geometries
- Design of non-wetting surfaces

Today’s readings

Nominal: (on ctools)

- Couchman and Jesser, “Thermodynamic theory of size dependence of melting temperature in metals”
- Goldstein et al., “Melting in semiconductor nanocrystals”
- Tuteja et al., “Design parameters for superhydrophobicity and superoleophobicity”

Surface energy (γ)

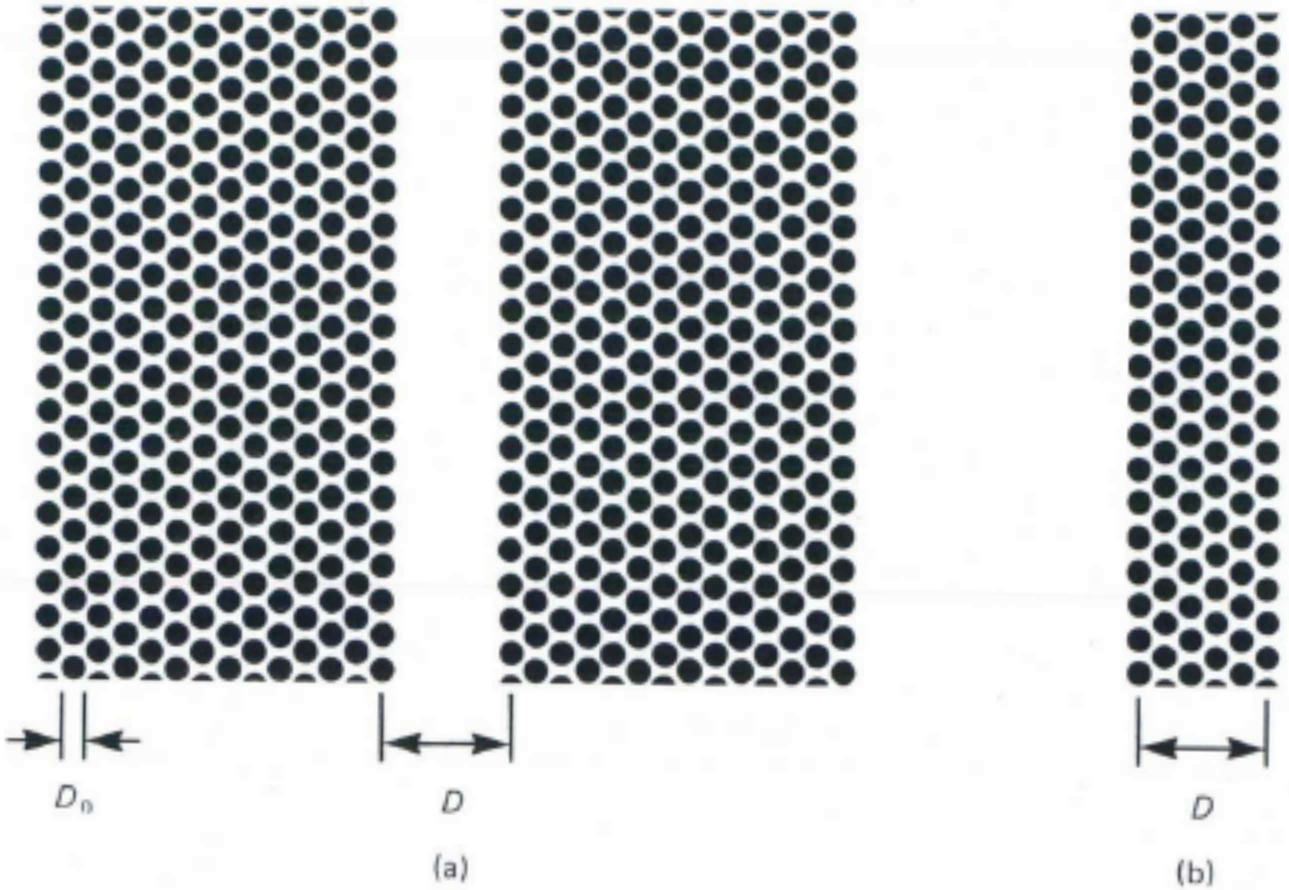

(a)

(b)

Fig. 11.8. (a) Two planar media or half-spaces. The pairwise summation of London dispersion energies between all atoms leads to Eq. (11.30). For two surfaces close together, their total surface energy may therefore be written as $2\gamma(1 - D_0^2/D^2)$. The long-range van der Waals interaction energy can be seen to be no more than a perturbation of the surface energy γ. A similar result is obtained for (b), a thin film.

Israelachvili.

total energy

$W = -(\cancel{\text{constant}})$ + energy of unsatisfied bonds on surface

$\uparrow$ bulk cohesive energy

$-(\text{vDW energy})$

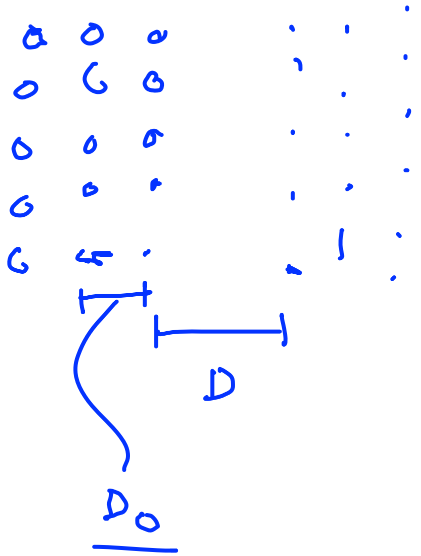

$$W = \frac{A}{12\pi}\left(\frac{1}{D_0^2}\right) - \frac{A}{12\pi}\left(\frac{1}{D^2}\right)$$

$$W = \frac{A}{12\pi D_0^2}\left(1 - \frac{D_0^2}{D^2}\right)$$ per unit area

$$\underline{D \gg D_0 \rightarrow W = \frac{A}{12\pi D_0^2} = 2\gamma},$$ γ = surface energy

$$\gamma = \frac{A}{24\pi\left(\sigma/2.5\right)^2}$$

D_0

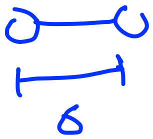

$\approx$ lattice parameter

surface energies typically much higher.

work of adhesion

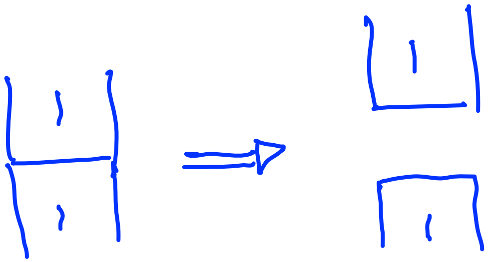

contact → ∞ separation

(vacuum)

$\underline{W_{11}} = \underline{2\gamma_{11}}$

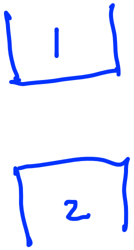

$$\gamma_{12} = \frac{1}{2}W_{11} + \frac{1}{2}W_{22} - W_{12} = \frac{1}{2}W_{121}$$

$$= \frac{1}{2}W_{212}$$

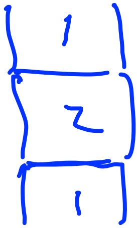

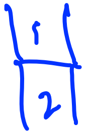

Surface energy across the periodic table

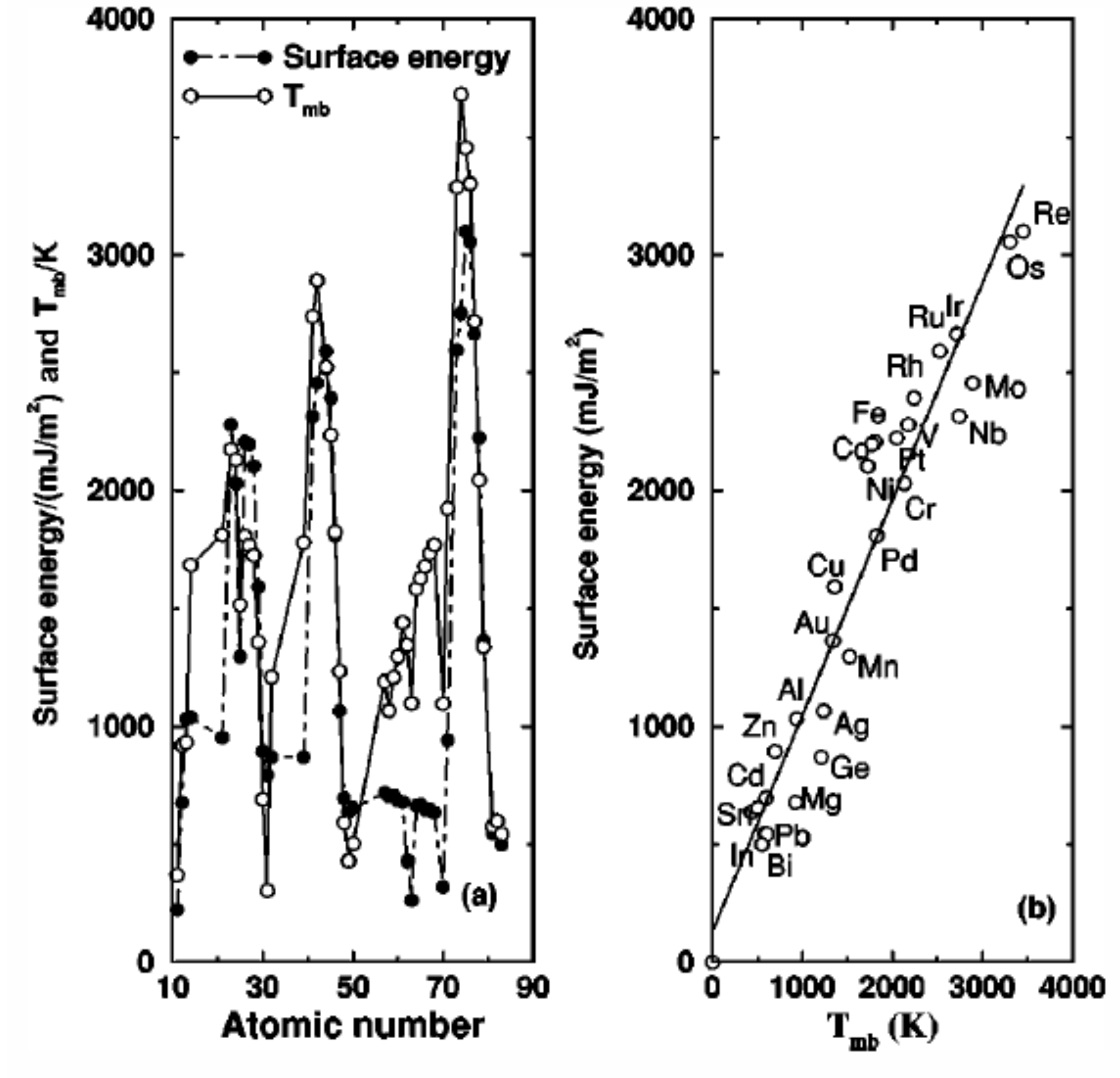

Nanda et al., Phys. Rev. B 66:013208, 2002.

Model of nanoparticle melting

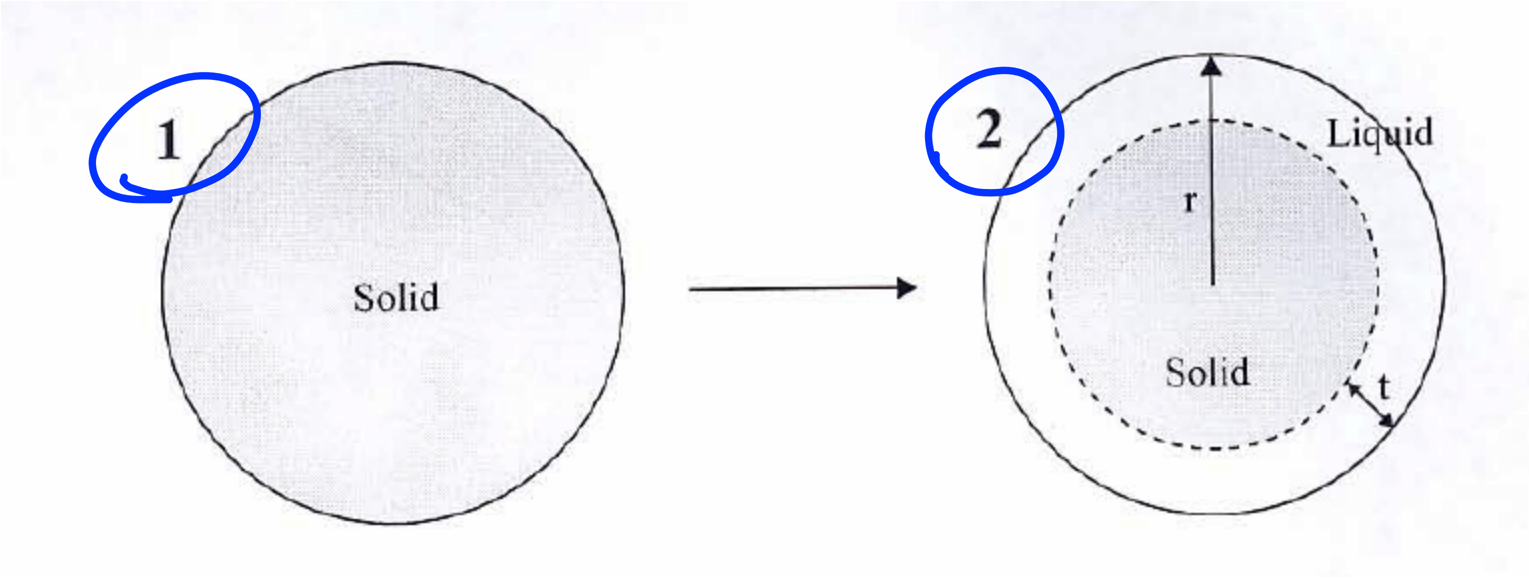

Assumptions:

- Spherical particle
- Melting begins at particle surface, with uniform liquid layer
- No volume or density changes
- Floating (no surrounding/substrate effects)

gibbs free energy: maximum mechanical work that can be extracted w/o volume Δ or heat transfer

$$\underline{dG} = \cancel{V\,dp} - \underline{S\,dT} + \cancel{\Sigma \mu_i\, dn_i}$$

$$\Delta G_{melting} = \underbrace{\Delta G^b}_{bulk} + \underbrace{\Delta G^s}_{surface}$$

$$\Delta G^b = G_2 - G_1 = V_\ell g_\ell + \underline{V_s g_s} - \underline{(V_\ell + V_s)} g_s$$

$$= V_\ell g_\ell + V_s g_s - \underline{V_t} g_s$$

↑ total volume of sphere

$$\Delta G^b = V_\ell \Delta g = V_\ell \underline{(g_\ell - g_s)}$$

by def. $$\left.\frac{dg}{dT}\right|_p = -s$$ ← entropy / volume

$$\Delta g = \int_{T_{M,b}}^{T} -s\,dT ,$$

$s(T)$ constant for each phase →

liquid : s^l

solid : s^s

latent heat of melting

$$\frac{h_0}{T_{Mb}}$$

$$\Delta g^l = (-s^l)(T - T_{Mb})$$

$$\Delta g^s = (-s^s)(T - T_{Mb})$$

$$\Delta g = \Delta g^l - g^s = \underline{(s^l - s^s)}(T_{Mb} - T)$$

$$\underline{\Delta g = \frac{h_0}{T_{Mb}}(T_{Mb} - T)}$$

$$\underline{\Delta G^b} = V_\ell \frac{h_0}{T_{mb}}\left(T_{mb}-T\right)$$

part 1

$$= \underbrace{\frac{4}{3}\pi\left(r^3-(r-t)^3\right)}\frac{h_0}{T_{mb}}\left(T_{mb}-T\right)$$

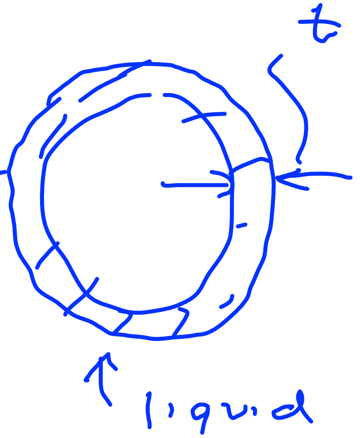

find ΔG^s

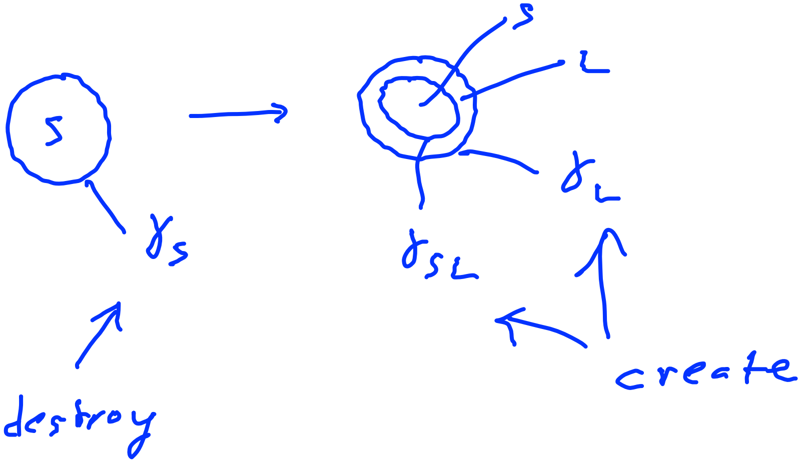

part 2

$$\underline{\Delta G^s} = 4\pi r^2\gamma_L + 4\pi(r-t)^2\gamma_{SL} - 4\pi r^2\gamma_s$$

$$= \underline{4\pi r^2(\gamma_L-\gamma_s) + 4\pi(r-t)^2\gamma_{SL}}$$

$$\Delta G^m = \Delta G^b + \Delta G^s$$

$$= \frac{4}{3}\pi \frac{h_o}{T_{mb}}(T_{mb} - T)\left(\cancel{r^3} - (r-t)^3\right)$$

$$+ \cancel{4\pi r^2(\gamma_L - \gamma_{SL}}) + 4\pi (r-t)^2 \gamma_{SL}$$

if $\frac{d\Delta G}{dt} < 0 \Longrightarrow$ particle will melt

$$\frac{d\Delta G}{dt} = +\cancel{3}\frac{\cancel{4}}{\cancel{3}}\cancel{\pi}\frac{h_o}{T_{mb}}(r-t)^{\cancel{2}}(T_{mb}-T) - 2\,\cancel{4\pi}\,\cancel{(r-t)}\,\gamma_{SL}$$

$$= 0 : \quad 2\gamma_{SL} = \frac{h_o}{T_{mb}}(r-t)(T_{mb}-T)$$

"critical thickness"

$$\boxed{t} = r - \frac{2T_{mb}\gamma_{SL}}{h_o(T_{mb}-T)}$$

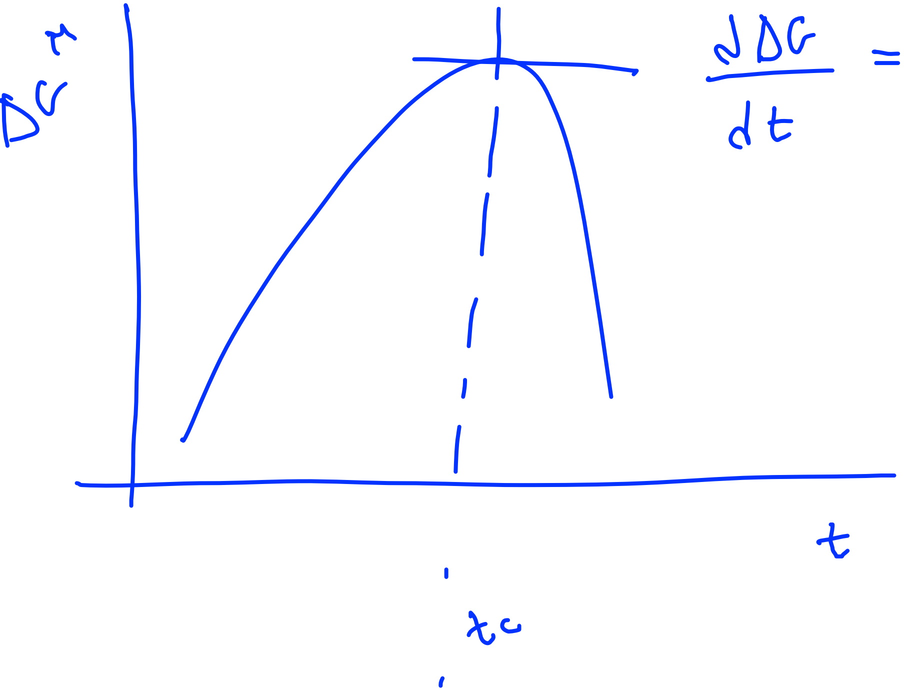

$$\frac{d\Delta G}{dt} = 0$$

Melts spontaneously

if $t_c \rightarrow 0$

$$\therefore \quad r = \frac{2 T_{Mb} \gamma_{sl}}{h_o (T_{Mb} - T)} \implies T_M = T_{Mb}\left(1 - \frac{2\gamma_{sl}}{h_o r}\right)$$

$$T_M = T_{Mb}\left(1 - \frac{C}{r}\right)$$

Fit of thermodynamic theory to data (Indium)

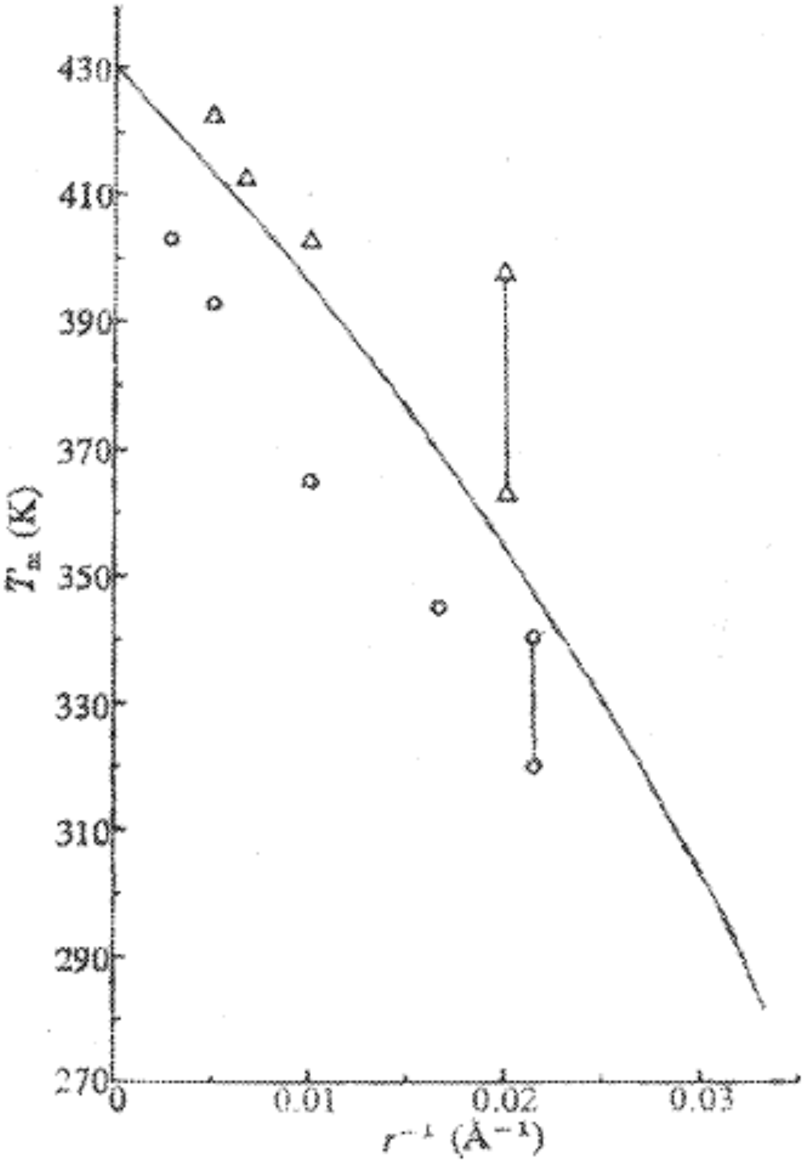

Couchman et al., Nature 269:481, 1977.

Is the catalyst solid or liquid?

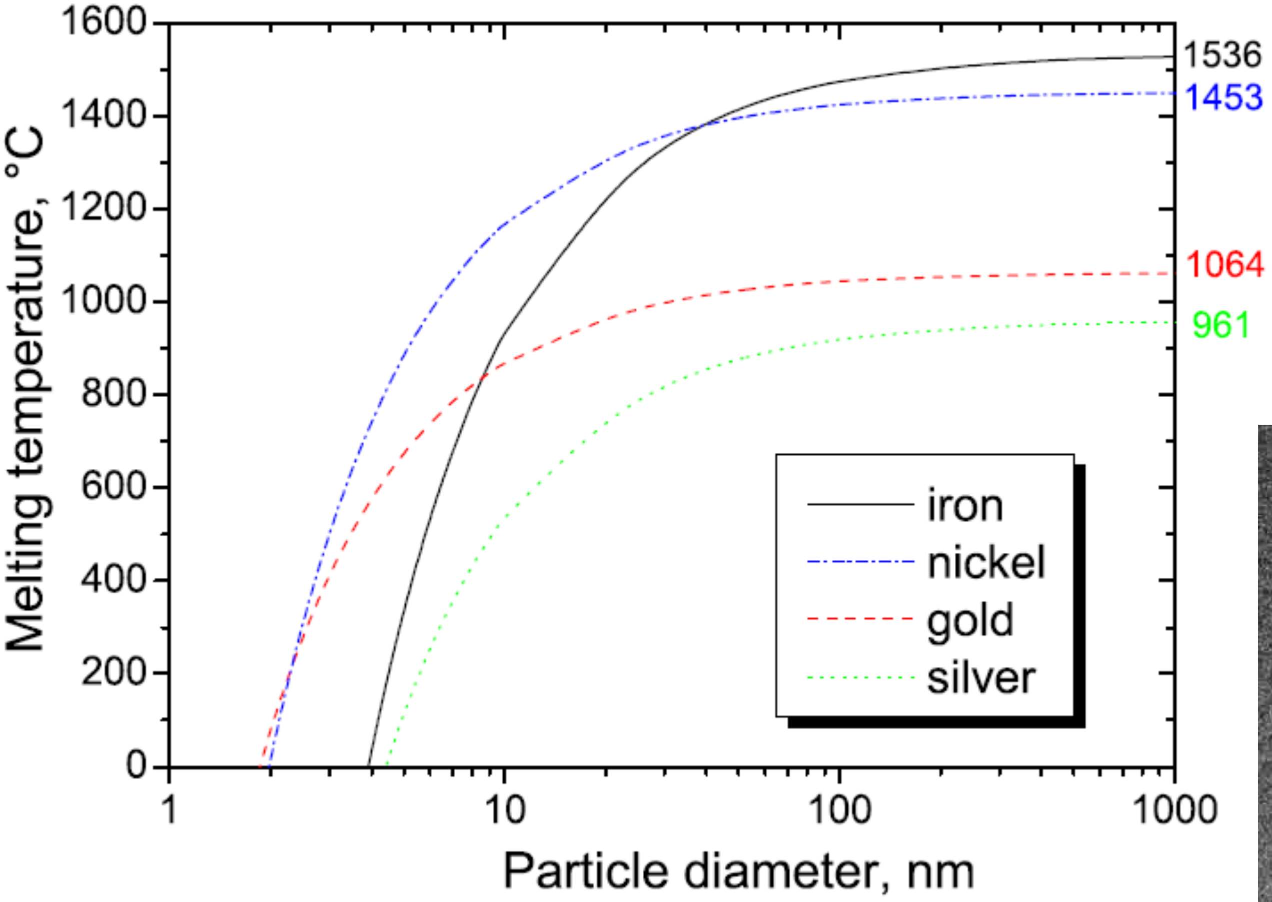

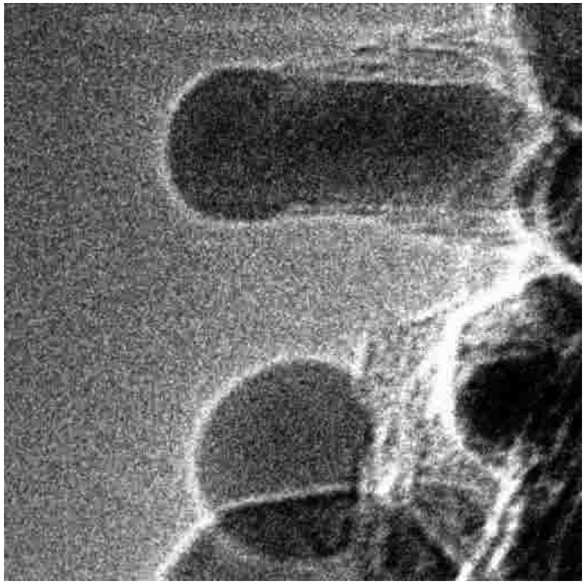

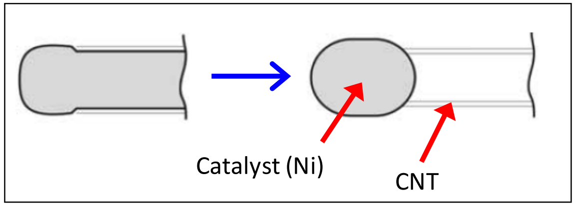

Moisala et al., *J. Phys. Cond. Matt.* 15:S3011, 2003.

Watching quantum dots melt

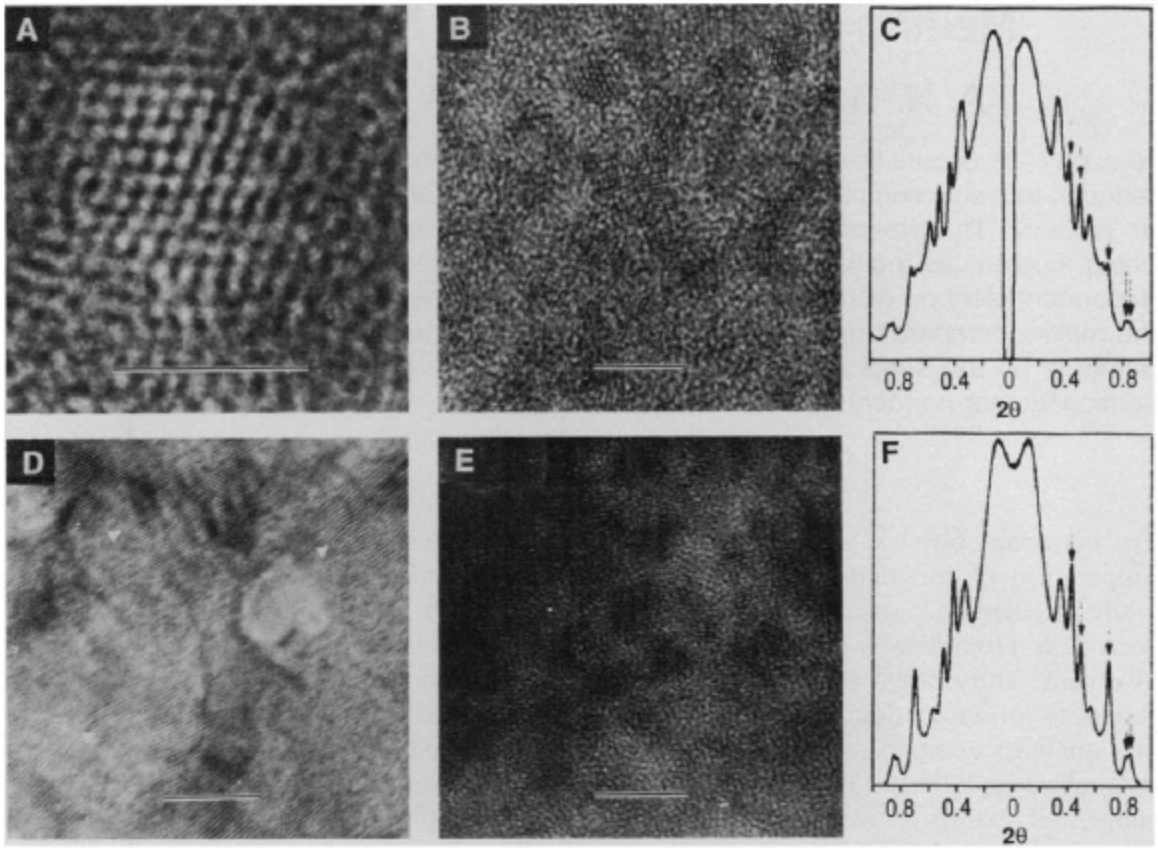

Fig. 1. The sequence of events during a melting experiment. The length marker in (A) is 30 Å; in the other panels the length marker represents 50 Å. (**A**) High-resolution micrograph of a single 30 Å CdS nanocrystal before heating. (**B**) Field of particles before heating. (**C**) The corresponding radially averaged ring diffraction pattern. (**D**) Polycrystalline thin film formed by melting and fusing nanocrystals in a region of high nanocrystal density on the grid [(111) planes are evident diagonally across the micrograph and can be seen along the directions of the white arrows]. (**E**) Field of isolated particles after a melting cycle. The shape and size are preserved from (B). (**F**) The diffraction pattern from isolated particles after melting shows increased crystallinity. The arrows in (C) and (F) denote the (111), (200), (220), (311), and (222) peaks of CdS. Peaks with no arrows above them are from the amorphous C substrate.

Goldstein et al., Science 256:1425, 1992.

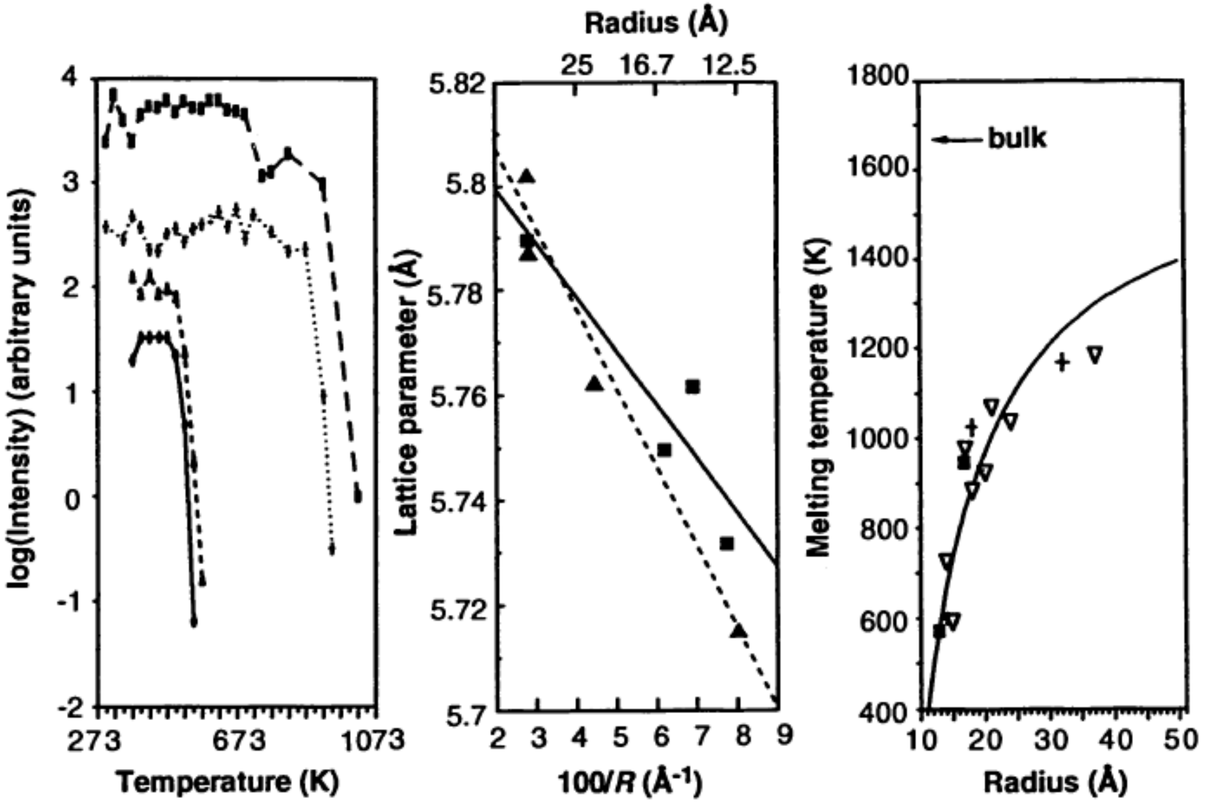

Fig. 2 (**left**). Logarithm of the intensity of electron diffraction from the (111) peak as a function of temperature for several sizes of CdS nanocrystals. The curves have been arbitrarily offset vertically for visual clarity. For each size, there is a sharp decrease in log intensity above the melting temperature. (◇ and solid line), 12 Å radius; (△ and short dashed line), 13 Å radius; (+ and dotted line), 16 Å radius; (■ and long dashed line), 18 Å radius. **Fig. 3** (**center**). Lattice parameter of CdS nanocrystals as a function of the reciprocal particle radius, *R*. (▲) Points from bare nanocrystals; the dashed line for bare nanocrystals yields a surface tension of 2.50 N m^{-1}. (■) Points from mercaptoacetic acid–capped nanocrystals; the solid line fit yields a surface tension of 1.74 N m^{-1}. **Fig. 4** (**right**). Size dependence of T_m for CdS nanocrystals. (■ and +) T_m derived from the disappearance of electron diffraction from an ensemble of thiophenol (or mercaptoacetic acid)–capped nanocrystals; (▽), T_m derived by observing the change in dark field of a single CdS particle. The solid curve represents a fit to Eq. 1 using γ_{sol} derived from Fig. 3.

Goldstein et al., Science 256:1425, 1992.

Magic numbers are more stable (Na)

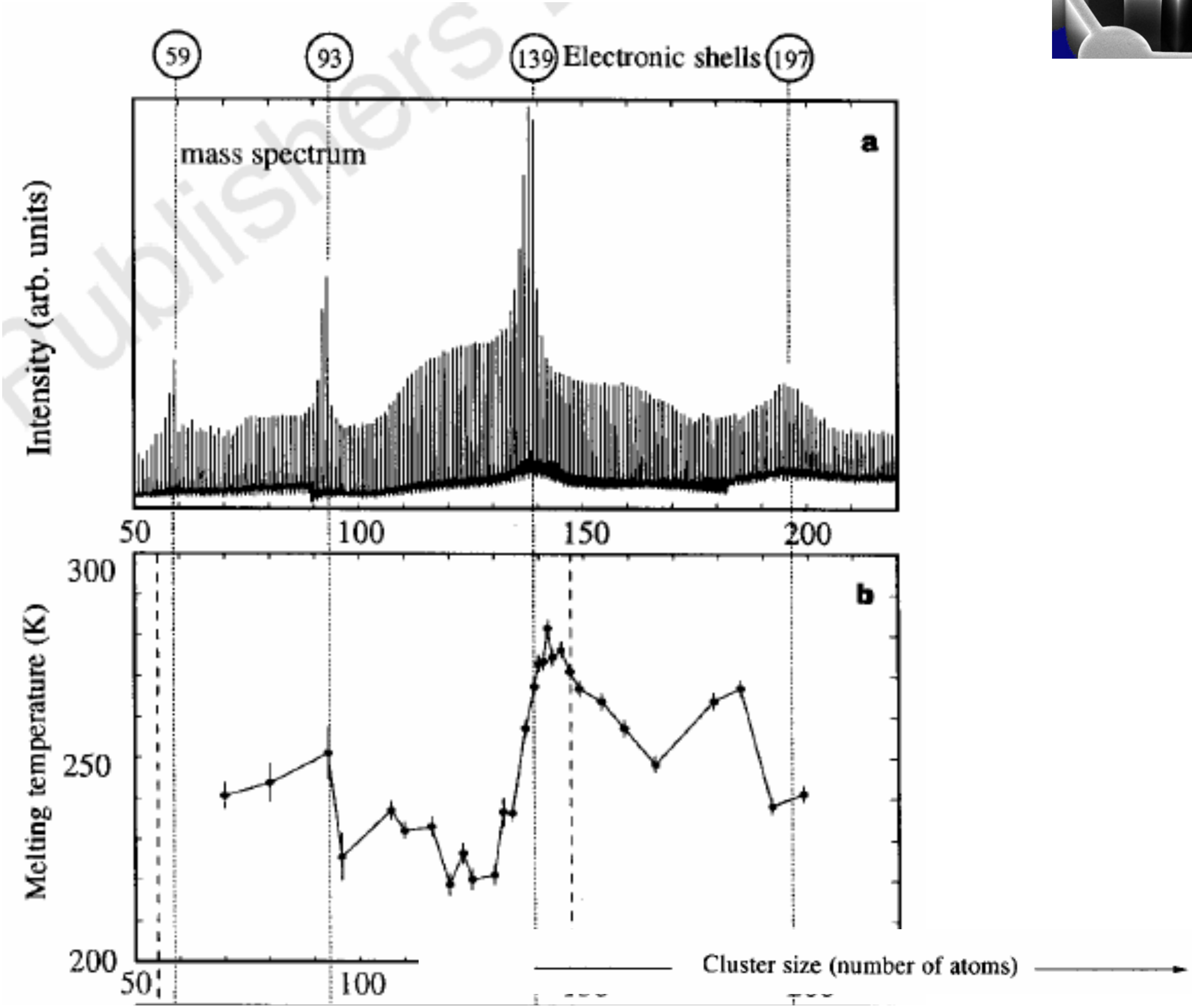

Schmidt et al., Nature 393:238, 1998.

$$T_m = T_{mb}\left(1 - \frac{c}{r}\right)$$

$$E_b = a_v N - (\text{surface area})\,\gamma$$

energy/atom

atoms

surface energy

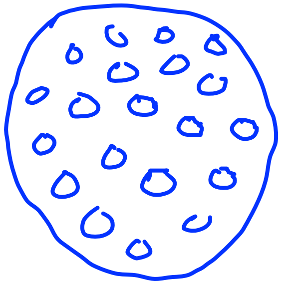

$$\frac{E_b}{N} = \underbrace{a_v}_{\text{bulk cohesive energy (per atom)}} - \frac{(SA)\,\gamma}{N} = a_{v,\,\text{nano}}$$

$$a_{v,np} = a_v - \frac{6\,\gamma\, v_a}{d}$$

sphere

atomic volume

diameter.

$$\frac{T_{M,nano}}{T_{Mb}} = 1 - \beta\left(\frac{SA}{Vol}\right)$$

⊖ 6/d

material properties

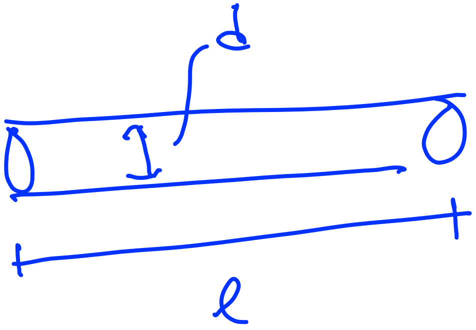

wire $\frac{SA}{V} = \frac{4}{d} + \frac{2}{l}$

if $l >> d$ $= \frac{4}{d}$

film

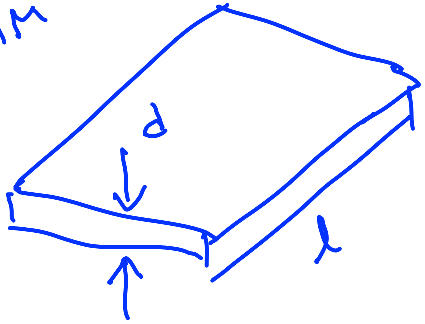

$\frac{SA}{V}$, if $l >> d$ $= \frac{2}{d}$ ← film thickness

$\frac{T_{Mb} - T_{M,nano}}{T_{Mb}}$: 3 : 2 : 1

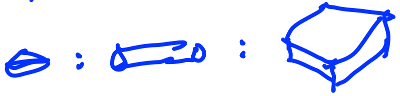

Dimensionality effect: wires vs. spheres

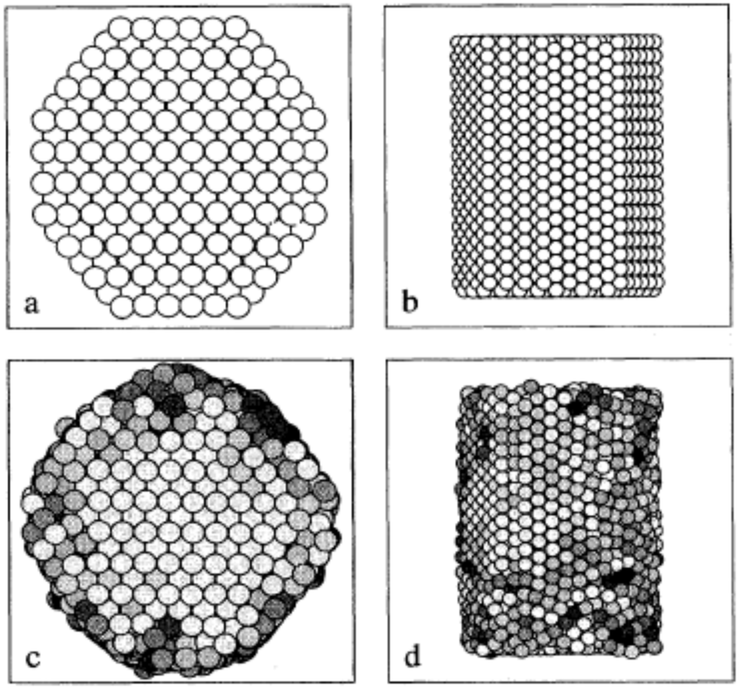

FIG. 1. Snapshot views of the MD sample with $N = 3294$ and $R \simeq 22.5$ Å. (a) and (b) are the initial sample at 0 K. (a) is the top view of the wire cross section. Wire axis (*z* direction) is perpendicular to this cross section. (b) is the side view from an angle such that all different laterals are seen. (c) and (d) are corresponding views at a temperature just below the melting temperature. The grayness of each atom is proportional to its square displacement during a MD run. White indicates a nondiffusing, crystalline behavior.

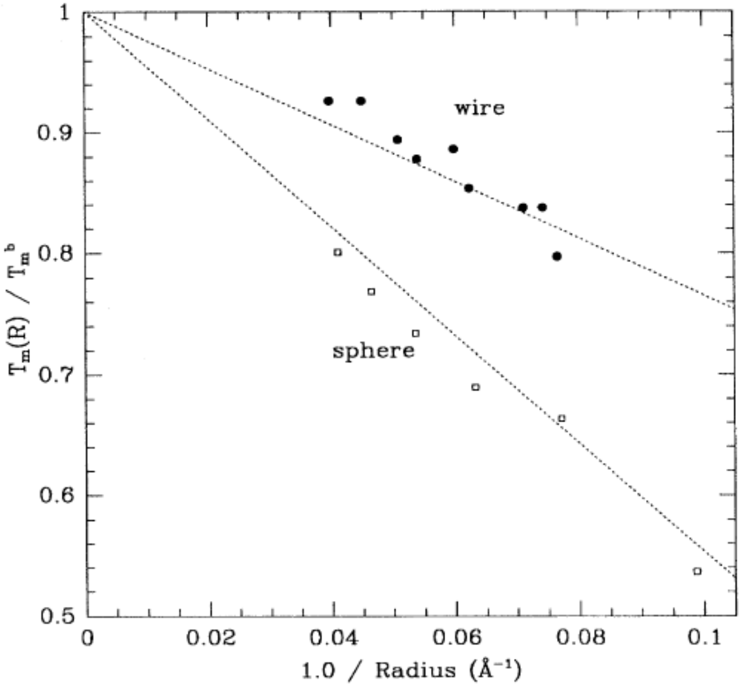

FIG. 3. Melting temperature of different clusters as a function of inverse radius. Solid circles refer to wires, open squares to spherical clusters, the dashed lines are the predictions of the simple phenomenological theory (see text).

Gulseren et al., Phys. Rev. B. 51(11):7337, 1995.

Hydrophilic or hydrophobic? (see videos)

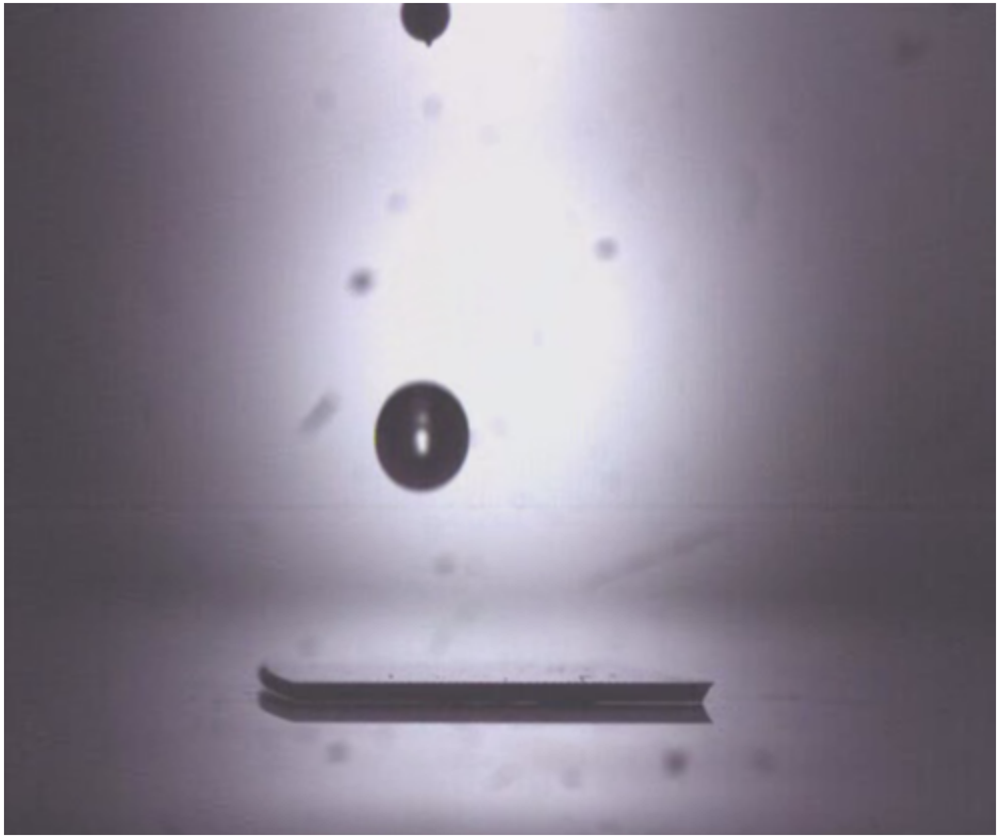

Courtesy of Hyungwoo Lee, MIT

Wetting

- Wetting is the ability of a liquid to maintain contact with a solid surface, resulting from intermolecular interactions when the liquid and solid are brought together
- Thus, the degree of wetting is determined by a force balance between adhesive and cohesive forces

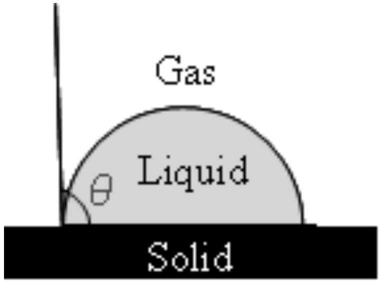

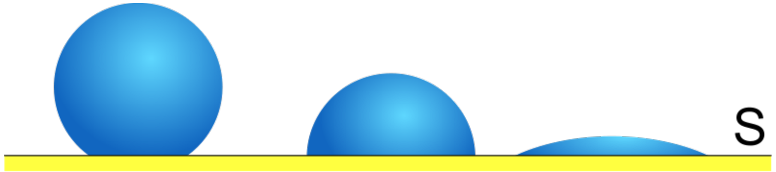

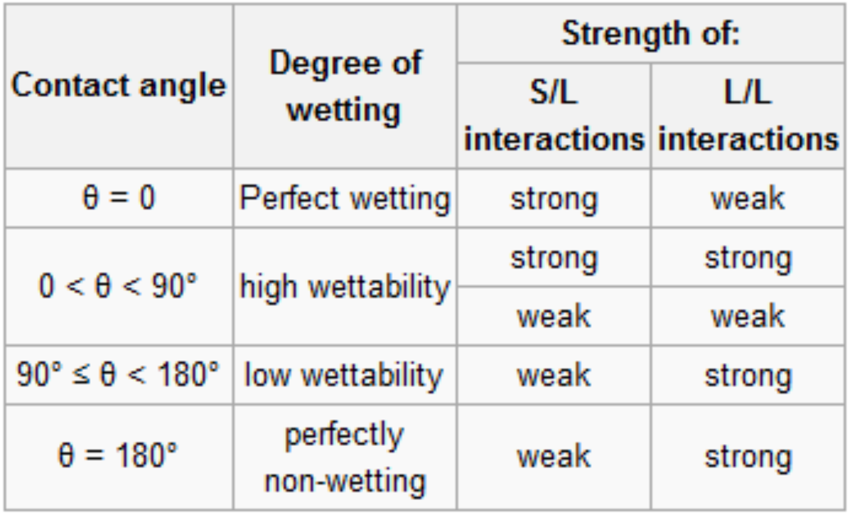

Contact angle	Degree of wetting	Strength of:	
		S/L interactions	L/L interactions
$\theta = 0$	Perfect wetting	strong	weak
$0 < \theta < 90°$	high wettability	strong	strong
		weak	weak
$90° \leq \theta < 180°$	low wettability	weak	strong
$\theta = 180°$	perfectly non-wetting	weak	strong

- Liquids more frequently wet solids having high surface energy (i.e., strongly bonded solids) than solids with low surface energy (i.e., VDW solids). It's practically difficult to prevent low surface energy liquids from wetting solids.

Textured surfaces: Cassie and Wenzel states

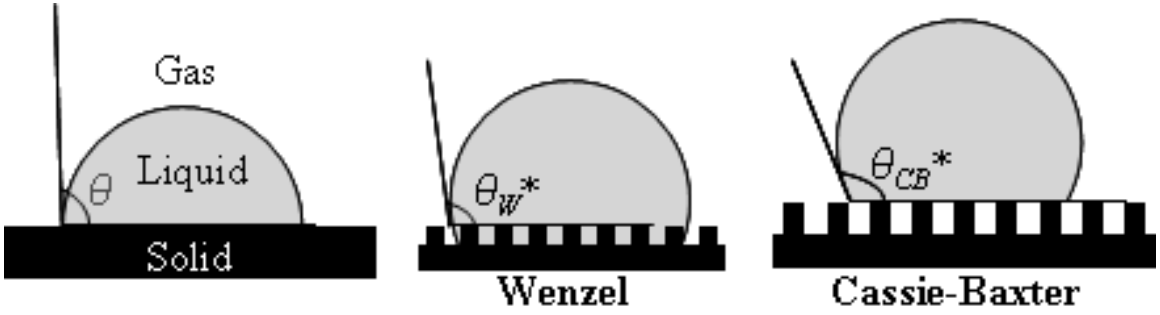

Advancing and receding contact angles –multiple stable contact angles

14-µm diameter, 30-µm height,and 105-µm pitch pillars

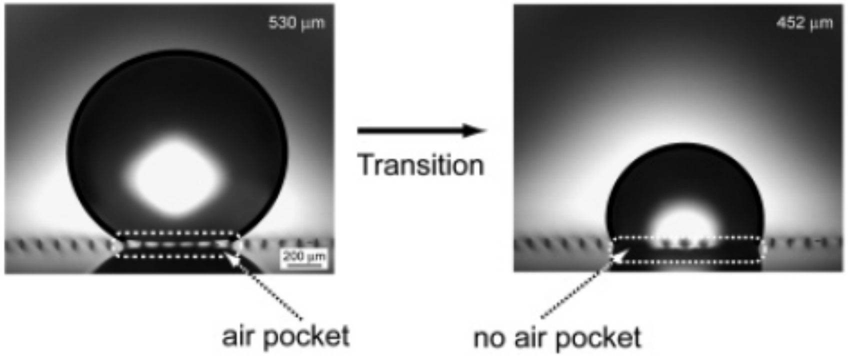

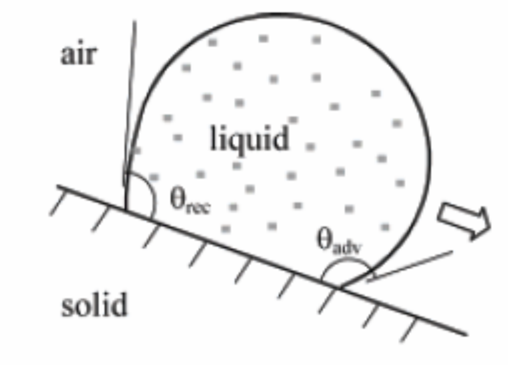

Droplet condensation and growth in ESEM

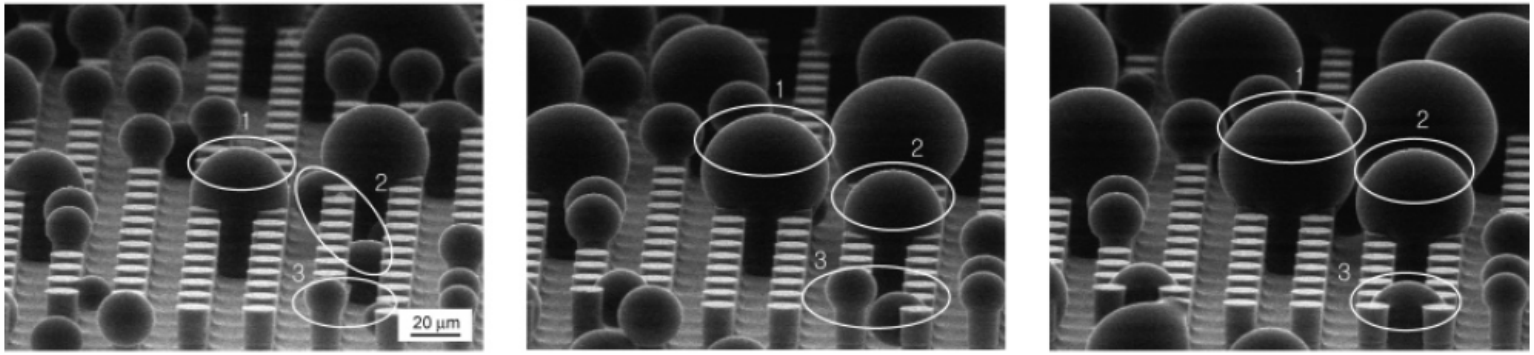

Water droplets in 1, 2, 3 appear

Water droplets in 2 merge

Water droplets in 3 merge

Nosonovsky and Bhusan, Nano Letters 7(9):2633-2637, 2007.

Superhydrophobicity: petal and lotus effects

- Rose petals and lotus leaves are both superhydrophobic; however, droplets roll off lotus leaves but do not roll off rose petals

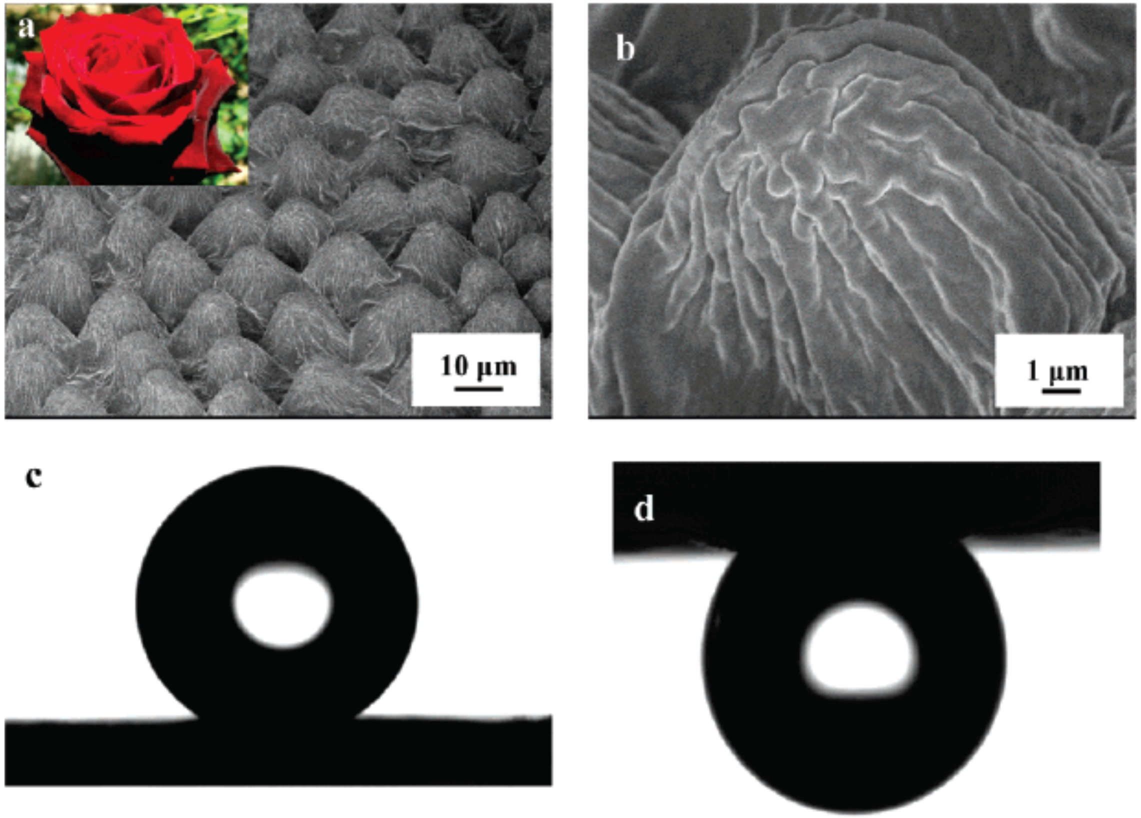

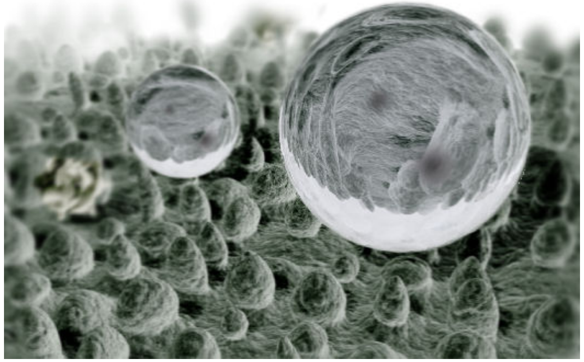

Feng et al., Langmuir 24(8):4114-4119, 2008.

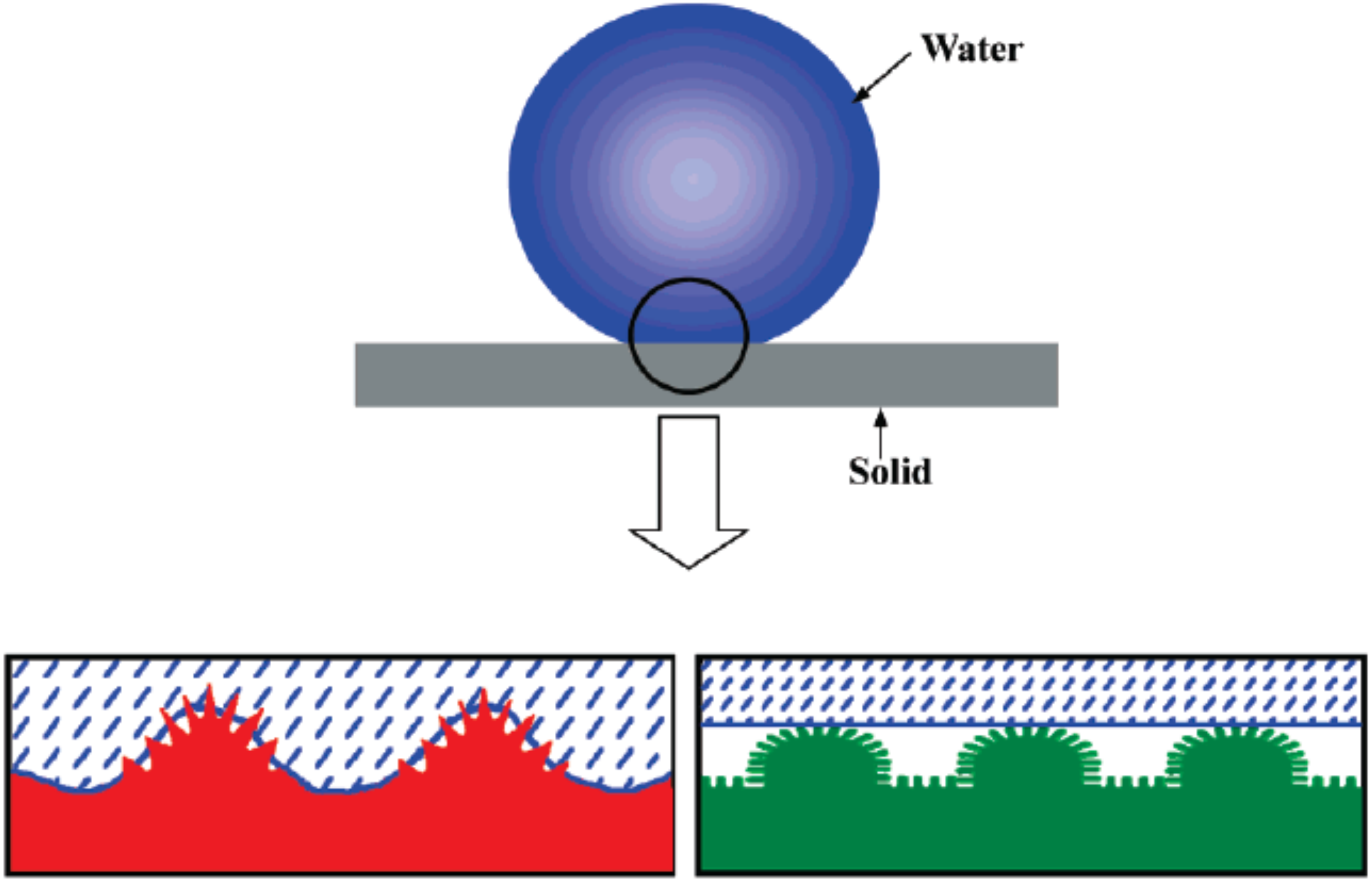

Petal (Cassie impregnating wetting state) **Lotus (Cassie's state)**

Figure 3. Schematic illustrations of a drop of water in contact with the petal of a red rose (the Cassie impregnating wetting state) and a lotus leaf (the Cassie's state).

Feng et al., Langmuir 24(8):4114-4119, 2008.

Texture + chemistry: PTFE-coated CNT forest

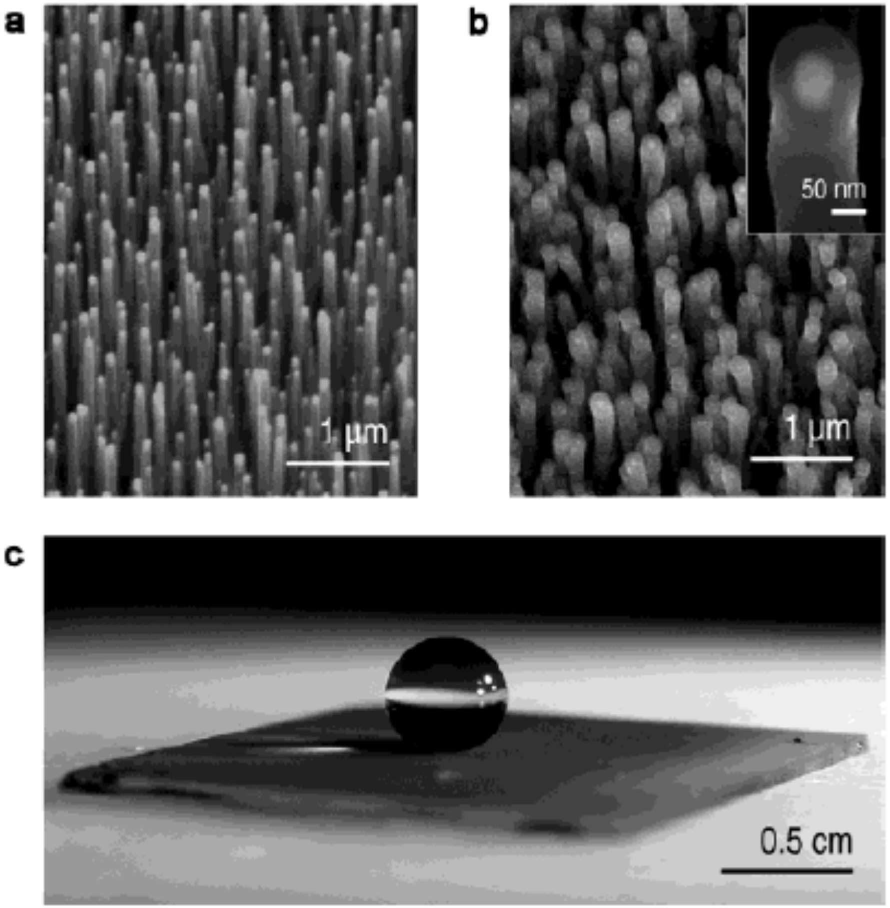

Figure 1. SEM images of carbon nanotube forests. (a) As-grown forest prepared by PECVD with nanotube diameter of 50 nm and a height of 2 μm, (b) PTFE-coated forest after HFCVD treatment, and (c) an essentially spherical water droplet suspended on the PTFE-coated forest.

Lau et al., Nano Letters 3(12):1701-1705, 2003.

Apparent contact angle of microstructures

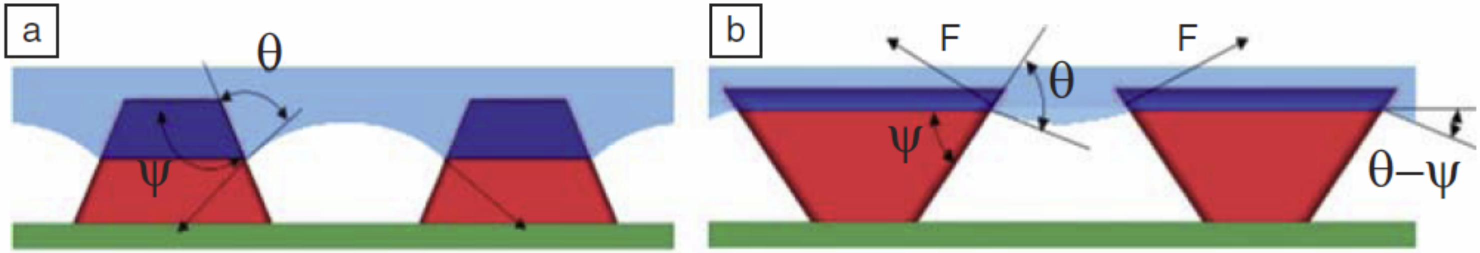

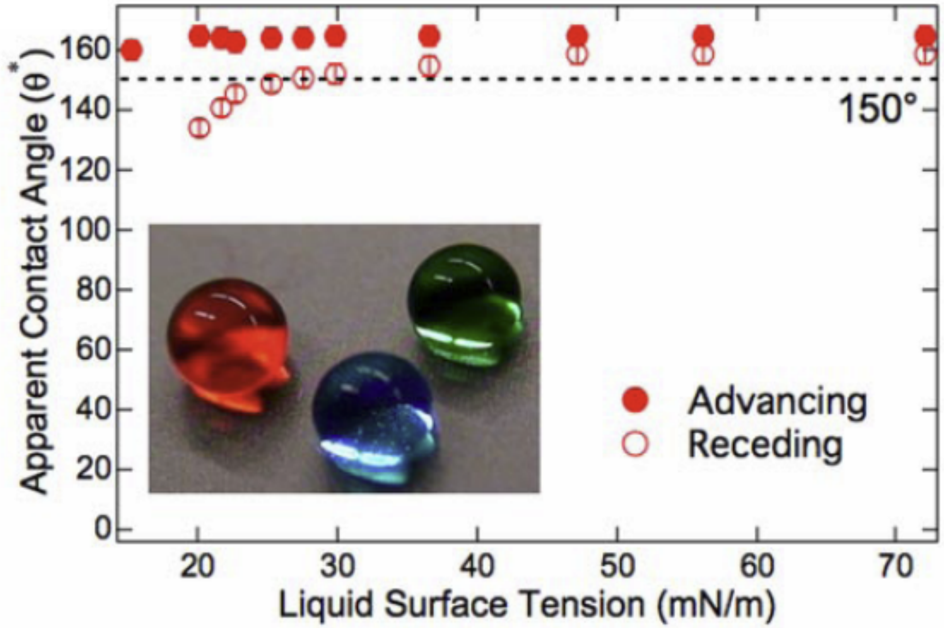

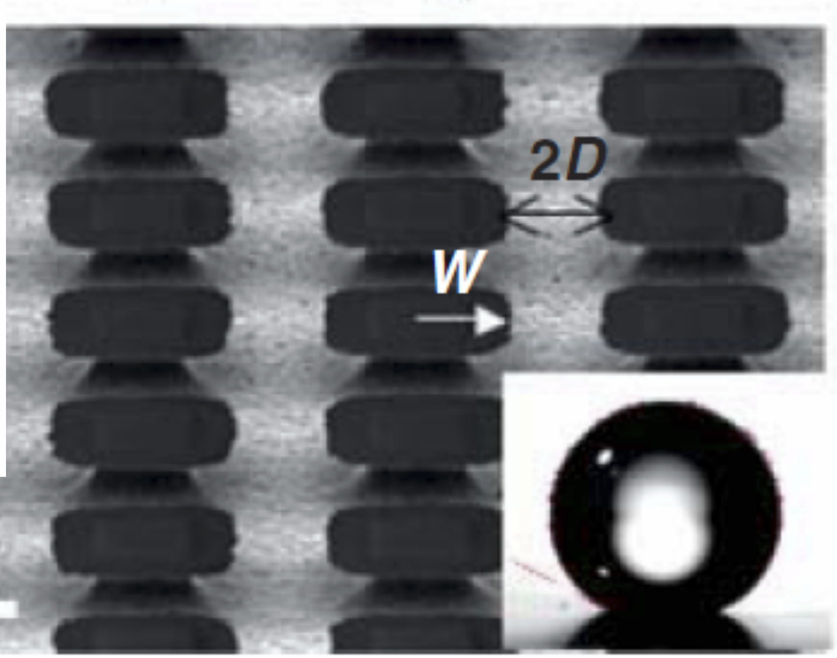

Tuteja et al., MRS Bulletin 33:752-758, 2008.
Tuteja et al., PNAS 105(47):18200-18205, 2008.